Structural distortion and orbital ordering in the triangular-lattice antiferromagnet $NaVO_2$ from first principles

Z. W. Ouyang,* N. M. Xia, S. S. Sheng, J. Chen, and Z. C. Xia
Wuhan National High Magnetic Field Center, Huazhong University of Science and Technology, Wuhan 430074, People's Republic of China

G. H. Rao
Beijing National Laboratory for Condensed Matter Physics, Institute of Physics, Chinese Academy of Sciences, Beijing 10080, People's Republic of China

X. H. Zheng
Key Laboratory of Materials Physics, Institute of Solid State Physics, Chinese Academy of Sciences, Hefei 230031, People's Republic of China

(Received 17 October 2010; revised manuscript received 3 January 2011; published 16 March 2011)

Triangular-lattice antiferromagnets with the general formula ATO_2 (A = alkali metal, $T = 3d$ transition metal) often adopt a slightly distorted crystal structure at low temperatures, accompanying a lifting of magnetic frustration and the appearance of long-range magnetic ordering and sometimes a particular orbital ordering. Taking $NaVO_2$ as an example, we successfully demonstrate that the tiny structural distortion with a ratio of lattice parameters, $a_m/b_m = 1.755$, and the formation of orbital ordering observed in recent neutron-diffraction experiments can be well interpreted by first-principles calculations including $3d$ electron correlations with parameter $U_{\text{eff}} = 3.6$ eV. This distinct study on "pure" structural distortion is expected to be applied in other triangular-lattice antiferromagnetic systems.

DOI: 10.1103/PhysRevB.83.094417 PACS number(s): 75.50.Ee, 71.20.−b

I. INTRODUCTION

Geometrical frustration, which stems from the topological arrangements of spins, is an important and intriguing phenomenon in magnetism.[1–7] Particularly interesting are the triangular-lattice systems composed of magnetic ions, in which once the first two spins are aligned antiparallely, the third one cannot simultaneously minimize its antiferromagnetic (AFM) interactions with both of the other two spins, giving rise to highly degenerate ground states. Such ground-state degeneracy, that is, magnetic frustration, may yield unconventional magnetic behavior, for example, spin-disordered liquid.[2–4]

In the triangular-lattice systems, the transition-metal-based oxides with the general formula ATO_2 (A = alkali metal, $T = 3d$ transition metal) are particularly interesting in both applications and fundamental physics. In additional to the large thermoelectric effect,[8–10] these compounds also exhibit a variety of unusual behavior, such as superconductivity,[11,12] charge-ordered insulator and "Curie-Weiss metal,"[13] unconventional dynamics and frustration,[14,15] and superparamagnetism and trimerization.[16] It is generally accepted that all these properties are related to the distinct quasi-two-dimensional triangular lattice formed by magnetic $3d$ ions. In such systems, long-range AFM ordering is prohibited due to strong magnetic frustration. At low temperatures, these systems tend to decrease its symmetry by a tiny structural distortion accompanying a reduction in the energy of the system. As a result, the magnetic frustration is removed and the system may favor a particular ground state sometimes with an orbital ordering.[17–21] For instance, α-$NaMnO_2$ crystallizes in the monoclinic structure ($C2/m$) due to the strong Jahn-Teller effect of Mn^{3+} ions,[22–24] resulting in the easing of geometrical frustration and a cooperative ferro-orbital ordering of the $d_{3z^2-r^2}$ orbital in the distorted MnO_6 octahedra.[25] Below ~45 K, the magnetic frustration is further lifted through a tiny monoclinic-triclinic structural phase transition simultaneously with an onset of long-range AFM ordering.[19,20,26] In the other analogous compound $NaVO_2$, a second-order rhombohedral-monoclinic structural transition takes place around 98 K with the appearance of orbital ordering of one electron per V^{3+} ion.[21] Below 93 K, the compound undergoes a first-order lattice distortion within the monoclinic phase along with an orbital ordering of two electrons per V^{3+} ion. Geometrical frustration is therefore relieved by these two successive orbital ordering transitions, and a long-range AFM ordering develops. Obviously, these examples present quite a different behavior from the other ATO_2 compounds, for example, $LiVO_2$ (Ref. 27) and $NaTiO_2$,[28] where a single transition to a nonmagnetic low-temperature phase was observed in the former and the exact nature of the observed transition is controversial in the latter.

Theoretically, Jia *et al.*[29] studied the ground state of $NaVO_2$ by comparing the total energies of several AFM configurations at fixed temperatures, but the structural stability at different temperatures, that is, 20, 91.5, and 100 K, was left without discussion. Indeed, the crystal structures at these temperatures are very close to each other and it might be difficult to determine which structure is more stable only by comparing their total energies. In this paper, we successfully demonstrate the small structural distortion as well as the orbital ordering observed in $NaVO_2$ by first-principles calculation. These results, combined with our prior work on α-$NaMnO_2$,[26] suggest that our study on structural distortion can be generalized to other triangular-lattice AFM systems.

This paper is organized as follows. The computational method is described briefly in Sec. II. The results and discussion are presented in Sec. III, which consists of four subsections: lattice-distortion calculations (Sec. III A), the process of lattice distortion and its correlation with magnetism (Sec. III B), density of states and orbital ordering (Sec. III C), and a comparison of $NaVO_2$ with other ATO_2 compounds (Sec. III D). Finally, we summarize our conclusion in Sec. IV.

II. COMPUTATIONAL METHOD

All calculations were carried out using the self-consistent full-potential linearized augmented-plane-wave package WIEN2K (Ref. 30) based on density-functional theory, using the general-gradient approximation (GGA) with the Perdew-Burke-Ernzerhof parametrization for the exchange correlation.[31] For the AFM state, the GGA + U calculations were also performed to include the correlations of 3d electrons. Since the value of U_{eff} of $NaVO_2$ is not available in the literature, we employ the value of isostructural $LiVO_2$, that is, $U_{\text{eff}} = U - J = 3.6$ eV (U and J are on-site Coulomb and exchange interactions, respectively).[29,32] Figure 1 shows the crystal and magnetic structures observed in neutron-diffraction experiments.[21,29] Since the interlayer V-V distance (~5.6 Å) is much greater than the intralayer one (~3.0 Å), $NaVO_2$ can be regarded as a pseudo-two-dimensional system. Brillouin-zone integrations were performed using 500 k points within the first Brillouin zone. The self-consistency is achieved when the convergence of total energy is smaller than 1 meV. The optimization of the internal parameters at 20 K, which will be used for the lattice-distortion calculations, shows that the sites of O atoms are (0.2358, 0, 0.7073), (0.2345, 0, 0.7045), and (0.2334, 0, 0.7088) for the nonmagnetic, FM, and AFM calculations, respectively, basically close to the experimental value.[21,29]

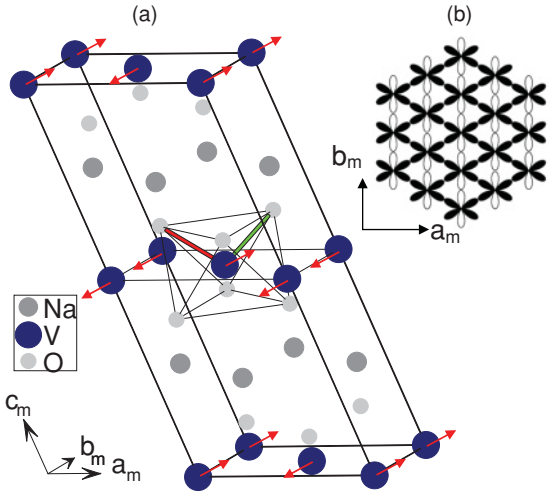

FIG. 1. (Color online) The crystal and magnetic structures (a) and the orbital ordering within the $a_m b_m$ plane (b) observed in neutron-diffraction experiments.[21] The long and short V-O bonds are shown, respectively, by red and green bonds. The filled lobes stand for the occupied d_{zx} and d_{yz} orbitals along the [110] and [1$\bar{1}$0] directions; the unfilled lobes are the less occupied d_{xy} orbital along the [010] direction.

III. RESULTS AND DISCUSSION

A. Lattice-distortion calculations

The lattice parameters and volume per formula unit observed in neutron-diffraction experiments[21,29] are listed in Table I. The rhombohedral lattice parameters at 100 K can be converted into $a_m = 5.1891$ Å, $b_m = a_m/1.732 = 2.9959$ Å, $c_m = 5.6384$ Å, and $\beta = 107.865^\circ$ in the monoclinic representation. Thus, it is very clear that the differences in crystallographic structure between 20, 91.5, and 100 K are quite small. Table I lists the total energies (E) calculated in different magnetic configurations, where the value of E corresponding to the AFM state at 20 K is taken as zero energy. As can be seen, for a fixed temperature the value of E in the AFM state is always lower than those of the nonmagnetic and FM states, in good agreement with previous results.[29] However, the energy differences between structures at different temperatures are a little complicated depending on the calculation methods. In the GGA case, the structure at 100 K has the lowest value of E for the FM and nonmagnetic states, whereas for the AFM state, the E of the 20 K structure is lowest. In the GGA + U ($U_{\text{eff}} = 3.6$ eV) calculation of the AFM state, the energy for the 100 K structure is lowest among these three temperatures, in contrast to the GGA calculation. Considering that the energy differences between different temperatures are not so pronounced (in particular, the difference between 20 and 100 K for the AFM state is so small that it is comparable to the calculation error) and such differences probably originate from a tiny deviation in structure as well as the unit-cell volume, it is indeed difficult to distinguish which structure is more stable in energy. This raises a question: What is the main aspect determining phase stability?

Note that the experimentally observed low-temperature long-range AFM ordering at 20 K is a result of the removal of the geometrical frustration in the layered triangular lattice. During this process, the equilateral triangles consisting of V ions in the rhombohedral phase at 100 K ($a_m/b_m = 1.732$) are distorted into isosceles triangles at 91.5 K ($a_m/b_m = 1.721$) and 20 K ($a_m/b_m = 1.755$), respectively (see Table I).[21,29] Thus, it is desired to perform a "pure" lattice-distortion calculation by ruling out the influences from the other structural parameters. More exactly, we start from the experimental lattice parameters at 20 K (Table I) and search for the possible energy minima by varying only a_m/b_m, simultaneously keeping c_m, angles, and volume unaltered. Figure 2 shows the a_m/b_m dependence of total energy relative to the value of $a_m/b_m = 1.755$. In the GGA calculation, the E-a_m/b_m curve for the nonmagnetic state exhibits a minimum around $a_m/b_m = 1.732$ (100 K) and a significant symmetry about this point [Fig. 2(a)]. This could be attributed to a higher geometrical symmetry of $a_m/b_m = 1.732$, at which V ions form equilateral triangles in the $a_m b_m$ plane and all the V-V distances are equal to each other (note that this is not the exact rhombohedral structure because the VO_6 octahedra are still distorted). In the FM calculation with GGA [Fig. 2(b)], the E-a_m/b_m curve exhibits a local maximum at $a_m/b_m = 1.721$, corresponding to the value at 91.5 K. Decreasing or increasing a_m/b_m, the energy decreases gradually until a local minimum around $a_m/b_m = 1.655$ and 1.750, with the former lower in energy than the latter. Although

TABLE I. Lattice parameters (Refs. 21 and 29), volume per formula unit, and calculated total energy (meV/f.u.) of $NaVO_2$ at 20, 91.5, and 100 K. The number marked by an asterisk is the value of a/b in the monoclinic representation.

Configuration	20 K	91.5 K	100 K
Structure	Monoclinic ($C2/m$)	Monoclinic ($C2/m$)	Rhombohedral (R-3m)
a (Å)	5.2223(2)	5.1758(1)	2.9959(1)
b (Å)	2.9755(1)	3.0078(1)	2.9959(1)
c (Å)	5.6492(3)	5.6340(1)	16.0996(1)
a_m/b_m	1.755	1.721	1.732*
β or γ (deg)	$\beta = 108.335(1)^\circ$	$\beta = 107.629(1)^\circ$	$\gamma = 120^\circ$
V (Å^3/f.u.)	41.665	41.975	40.715
GGA Nonmagnetic	304	316	287
FM	51	53	36
AFM	0	39	2.7
GGA + U AFM	0	33	−2.6

the physics behind the minimum around $a_m/b_m = 1.655$ is not clear at this moment, $a_m/b_m = 1.750$ nearly points to the experimental value of $a_m/b_m = 1.755$ at 20 K (Table I). For the AFM calculation with the GGA [Fig. 2(c)], the E-a_m/b_m curve exhibits only one minimum around $a_m/b_m = 1.767$, which is slightly larger than the experimental value at 20 K.

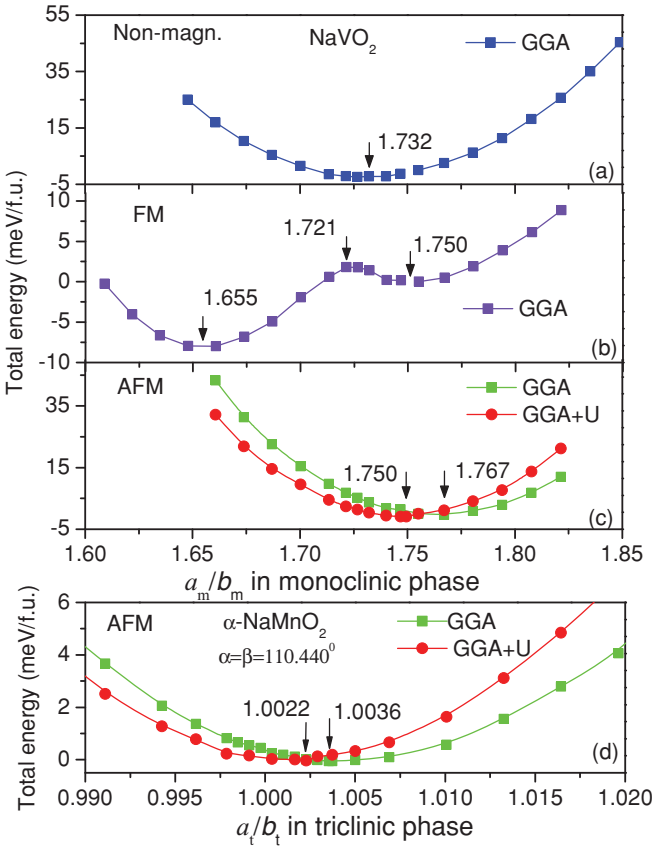

FIG. 2. (Color online) The E-a_m/b_m curves of $NaVO_2$ for nonmagnetic, FM, and AFM calculations (a)–(c). The E of experimental AFM monoclinic volume, V_{exp}, is taken as energy zero. The result for α-$NaMnO_2$ is also shown for comparison (d).

To further illustrate the stability of the monoclinic phase, we performed the GGA + U (U_{eff} = 3.6 eV) calculations for the AFM state, as is shown in Fig. 2. Compared with the result of the GGA calculation, the minimum of the E-a_m/b_m curve now moves to a lower value of $a_m/b_m = 1.750$, nearly pointing to the experimental monoclinic structure of $a_m/b_m = 1.755$ at 20 K. We note that the energy at $a_m/b_m = 1.750$ is lower than those at $a_m/b_m = 1.732$ and 1.721 by only 1–2 meV/f.u., which are comparable to the calculation errors. However, judging from the smooth E-a_m/b_m curve, we infer that the monoclinic structure with $a_m/b_m = 1.750$ is more stable than those of $a_m/b_m = 1.732$ and 1.721. Hence, our results not only demonstrate successfully the AFM ground state with $a_m/b_m = 1.750$, in good agreement with recent neutron-diffraction experiments,[21] but they also suggest that an inclusion of 3d electron correlations in the calculations is essential and $NaVO_2$ has almost the same value of U_{eff} as its sister compound $LiVO_2$.[32]

B. Process of lattice distortion and its correlation with magnetism

In addition to the prediction of the AFM ground state with $a_m/b_m = 1.750$, Fig. 2 also elucidates the process of lattice distortion as well as its correlation with magnetism. On the one hand, as an equilateral triangle consisting of V ions in the rhombohedral phase (R-3m) is distorted into an isosceles triangle in the monoclinic phase ($C2/m$), the geometrical symmetry of the compound is reduced. An introduction of magnetism, either FM or AFM, prompts such a reduction in symmetry due to magnetoelastic coupling. However, only the introduction of the AFM state can induce an experimentally observed lattice distortion. This tiny lattice distortion slightly lowers the energy of the system by removing the magnetic frustration and establishing low-temperature long-range AFM ordering. On the other hand, based on the requirement of energy reduction, the general rule for the rhombohedral-monoclinic distortion is $a_m/b_m > 1.732$. In this process, the original equal V-V bonds in the VO_2 layer split into two short bonds along the [010] direction and four long bonds along the [110] and [1$\bar{1}$0] directions. Defining the distortion of the

VO_6 octahedron as $(d_1-d_2)/d_2$, where d_1 and d_2 are the long and short V-O bond lengths, respectively [see Fig. 1(a)], will result in an enhancement of distortion of the VO_6 octahedron. Experimentally, however, a second-order structural transition from $a_m/b_m = 1.732$ (100 K) to 1.721 (91.5 K), in which the energy is increased, was indeed observed. This might show that the AFM state at $a_m/b_m = 1.721$ is a metastable intermediate state, in which the VO_2 layer is composed of two long bonds along the [010] direction and four short bonds along the [110] and [1$\bar{1}$0] directions. Concomitantly, the VO_6 octahedron is compressed along its axial direction. Such a state is not stable and can be converted into a more stable one with $a_m/b_m > 1.732$ by a discontinuous reversal of V-V bond length, as was observed in the first-order lattice distortion from $a_m/b_m = 1.721$ to 1.755,[21] during which the distortion varies discontinuously from -1.83% to $+2.40\%$. In addition, the first-principles calculation that is usually employed to predict the ground state (absolute zero temperature) might not be relied on to mimic the temperature-induced structure transition. To predict correctly the order of the phase transition, a detailed calculation on structural stability including thermodynamic properties such as enthalpies of formation, zero-point energy, and temperature-dependent free energy is desired.

C. Density of states and orbital ordering

We now examine how the density of states (DOS) varies with the lattice distortion. Figure 3 plots the total and projected DOS of $a_m/b_m = 1.721$, 1.732, and 1.750. The empty a_{1g} band is pushed upward and a gap of 1.5 eV is opened near the Fermi level, characterizing an insulator due to strong correlation of 3d electrons.[29] The total and projected DOS nearly overlap with each other because there are no dramatic changes in the occupation of d orbitals, the V-O bond lengths, and spin magnetic moment ($1.68\mu_B$/V). However, close scrutiny still reveals a slight increase in the occupation of d orbitals as

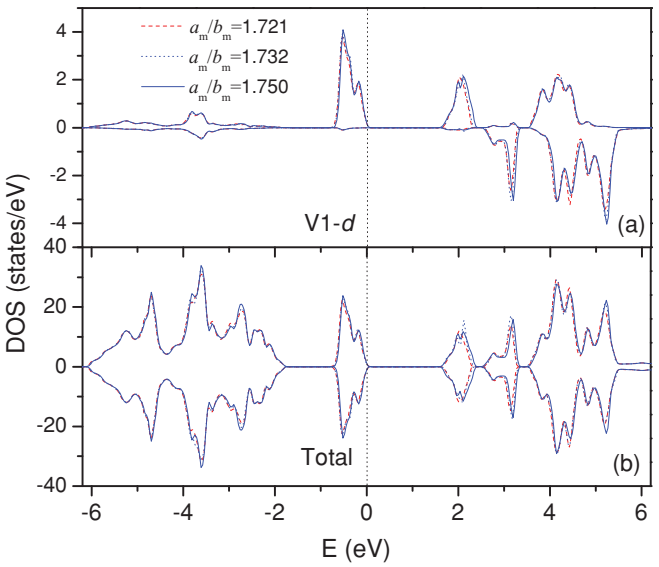

FIG. 3. (Color online) The total and projected DOS of the AFM state calculated by GGA + U ($U_{\text{eff}} = 3.6$ eV) for $a_m/b_m = 1.721$, 1.732, and 1.750.

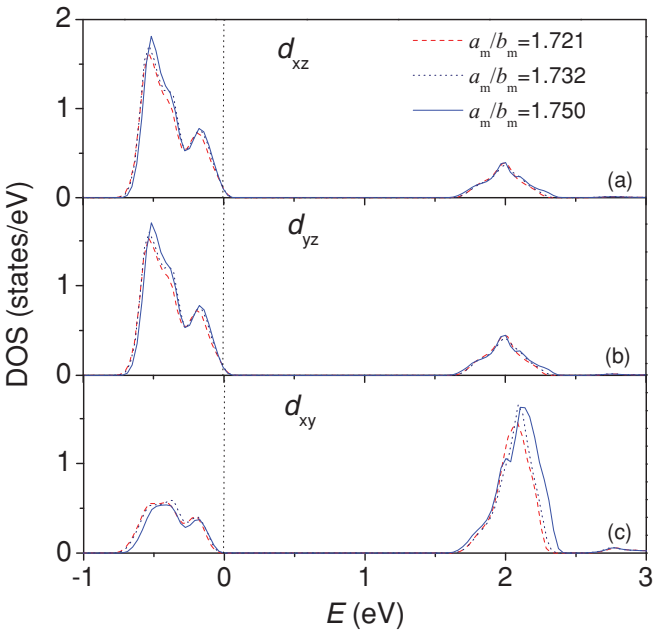

FIG. 4. (Color online) The spin-up DOS of d_{zx}, d_{yz}, and d_{xy} orbitals of V1 ion in local coordinate system. The calculations were performed for the AFM state by using GGA + U ($U_{\text{eff}} = 3.6$ eV).

the compound undergoes a distortion from $a_m/b_m = 1.721$ to 1.750.

To further explore the tiny variation of d-orbital occupation, Fig. 4 shows the spin-up DOS of d_{zx}, d_{yz}, and d_{xy} orbitals of the V1 ion in a local coordinate system, where the z axis of this system points to the V-O bond of the VO_6 octahedron.[29] It is clear that the d_{zx} and d_{yz} orbitals are mainly occupied and the d_{xy} orbital is less occupied at all V ions. Such a spatial distribution of 3d partial DOS is consistent with the Goodenough-Kanamori rules,[33,34] based on which the empty orbitals lie along the two short V-V bonds, favoring the FM exchange interaction along the [010] direction, whereas the filled orbitals lie along the four long V-V bonds, favoring the AFM interaction along the [110] and [1$\bar{1}$0] directions (see Fig. 1 for the AFM spin arrangement and orbital ordering of V ions within the $a_m b_m$ plane).[21] This is different from other vanadates, for example, $LaVO_3$, in which the orbital order violates the Goodenough-Kanamori rules due to spin-orbital entanglement.[35] Most interestingly, Fig. 4 also reveals that during the distortion from $a_m/b_m = 1.721$ to 1.750, the occupations of d_{zx} and d_{yz} orbitals are slightly enhanced, while that of the d_{xy} orbital exhibits a significant reduction. It is thus proposed that, ignoring the metastable intermediate state of $a_m/b_m = 1.732$ (see above), the experimentally observed lattice distortion is a result of the enhancement of the occupied d_{zx} or d_{yz} orbitals and the weakening of the less occupied d_{xy} orbital. The orbital ordering as well as its enhancement are a mechanism for driving the compound to distort from $a_m/b_m =$ 1.721 to 1.750, which relieves the magnetic frustration and stabilizes the long-range AFM ordering.

D. Comparison of $NaVO_2$ with other ATO_2 compounds

So far, we have successfully illustrated the experimentally observed AFM ground state, tiny lattice distortion, and

orbital ordering in $NaVO_2$ by a detailed lattice-distortion calculation. Since a similar method was applied in α-$NaMnO_2$,[26] here we compare both systems. The common factor is that both systems experience similar lattice distortion, that is, rhombohedral-monoclinic-triclinicdistortion in α-$NaMnO_2$,[19,20] and rhombohedral-monoclinic distortion in $NaVO_2$,[21,29] resulting in low-temperature long-range AFM ordering. Presumably because of this similarity, the lattice-distortion calculation can be well applied in both systems. Noting that the present AFM calculation of $NaVO_2$ using the GGA overestimates the energy minimum whereas the GGA + U calculation compensates for this deviation, we recalculate the monoclinic-triclinic distortion of α-$NaMnO_2$ by using GGA + U ($U_{\text{eff}} = 8.8$ eV),[25,36] which was not included previously.[26] The result shows that the energy minimum moves from $a_t/b_t = 1.0036$ to $a_t/b_t = 1.0022$ [see Fig. 2(d)], in surprisingly good agreement with the experimental value of $a_t/b_t = 1.0023$.[26] Thus, both systems show the importance of including $3d$ electron correlations. The values of U_{eff} obtained from the isostructural $LiVO_2$ (Ref. 32) for $NaVO_2$ and by the constrained local-density approximation[36] for α-$NaMnO_2$, respectively, are further confirmed.

The differences between both compounds are also pronounced. In α-$NaMnO_2$ with a strong Jahn-Teller Mn^{3+} ($t_{2g}^3 e_g^1$) ion, the orbital degeneracy is well lifted. As a result, the compound adopts a distorted monoclinic structure even at room temperature. The MnO_6 octahedra are axially elongated during this large hypothetical rhombohedral-monoclinicdistortion, accompanied by a large variation in the distortion-related energy (see Ref. 26). The elongated Mn-O bond points in the same direction as the cooperative ferro-orbital ordering of a $d_{3z^2-r^2}$ orbital in the $a_m c_m$ plane. Obviously, in such a strong Jahn-Teller system, the lattice distortion determines the type of orbital ordering. In $NaVO_2$, however, Jahn-Teller effect of V^{3+} ($t_{2g}^2 e_g^0$) is not that strong and the lifting of orbital degeneracy is more subtle.[32] It was proposed that peculiar orbital ordering can remove the geometric frustration and lower the energy of the system.[18] $NaVO_2$ manifests itself as such a system by showing two successive orbital ordering transitions.[21] The orbital ordering, which now lies in the $a_m b_m$ plane, removes the frustration, leading to small rhombohedral-monoclinic distortions along with a relatively smaller distortion-related energy [see Fig. 2(c)]. The VO_6 octahedra are compressed in the beginning followed by a later elongation, different from the uniform elongation of the Mn-O bond in α-$NaMnO_2$.

Finally, we point out that a similar lattice-distortion calculation might be applied in other ATO_2 compounds containing Jahn-Teller ions. For instance, $LiMnO_2$ was reported to have an orthorhombic ($Pmmn$) structure that is stabilized by AFM ordering.[37,38] This is different from α-$NaMnO_2$ and quite unusual since Li is isoelectronic to Na. The $NaTiO_2$ and $LiVO_2$ have nonmagnetic low-temperature phases, but the details are quite different and still controversial. $LiVO_2$ undergoes a first-order orbital ordering transition below 500 K, corresponding to the trimerization (or "clusters") of a V triangular lattice.[27,33] In contrast, $NaTiO_2$ exhibits a second-order rhombohedral-monoclinic transition below 250 K.[28] Both of these are different from $NaVO_2$. An intensive lattice-distortion calculation would be useful in elucidating the phase stability of these systems.

IV. CONCLUSIONS

Our first-principles study on triangular-lattice antiferromagnet $NaVO_2$ predicts a right monoclinic AFM ground state with a ratio of lattice parameters of $a_m/b_m = 1.750$, which is very close to the experimental observation. For this successful prediction, it is essential to include $3d$ electron correlations with parameter $U_{\text{eff}} = 3.6$ eV in the calculations. The lattice distortion is found to be strongly correlated with magnetism. It is the tiny lattice distortion that results in the removal of magnetic frustration and final onset of low-temperature long-range AFM ordering. In accordance with the Goodenough-Kanamori rules, the orbital ordering as well as its enhancement are identified as a mechanism for lattice distortion at low temperatures. The similarities and differences in the low-temperature lattice distortions between $NaVO_2$ and α-$NaMnO_2$ are discussed. Our study on structural distortion offers a distinct way to study the phase stability of frustrated triangular-lattice antiferromagnets. In particular, this method may be useful to understand the phase stability of some other ATO_2 compounds, for example, $LiMnO_2$, $NaTiO_2$, and $LiVO_2$.

ACKNOWLEDGMENTS

We thank G. R. Zhang and T. Jia for discussions. This work is supported by Scientific Research Foundation for Returned Scholars (No.0124012014), Huazhong University of Science and Technology.

*Author to whom all correspondence should be addressed: zwouyang@mail.hust.edu.cn

[1] M. F. Collins and O. A. Petrenko, Can. J. Phys. **75**, 605 (1997).
[2] R. Coldea, D. A. Tennant, A. M. Tsvelik, and Z. Tylczynski, Phys. Rev. Lett. **86**, 1335 (2001).
[3] Y. Shimizu, K. Miyagawa, K. Kanoda, M. Maesato, and G. Saito, Phys. Rev. Lett. **91**, 107001 (2003).
[4] S. Nakatsuji, Y. Nambu, H. Tonomura, O. Sakai, S. Jonas, C. Broholm, H. Tsunetsugu, Y. Qiu, and Y. Maeno, Science **309**, 1697 (2005).
[5] S. -H. Lee, H. Kikuchi, Y. Qiu, B. Lake, Q. Huang, K. Habicht, and K. Kiefer, Nature Mater. **6**, 853 (2007).
[6] S. Yoshii, K. Ohoyama, K. Kurosawa, H. Nojiri, M. Matsuda, P. Frings, F. Duc, B. Vignolle, G. L. J. A. Rikken, L. P. Regnault, S. Michimura, and F. Iga, Phys. Rev. Lett. **103**, 077203 (2009).
[7] Y. Machida, S. Nakatsuji, Y. Maeno, T. Tayama, T. Sakakibara, and S. Onoda, Phys. Rev. Lett. **98**, 057203 (2007).
[8] A. R. Armstrong and P. G. Bruce, Nature (London) **381**, 499 (1996).
[9] I. Terasaki, Y. Sasago, and K. Uchinokura, Phys. Rev. B **56**, 12685(R) (1997).

[10]Y. Y. Wang, N. S. Rogado, R. J. Cava, and N. P. Ong, Nature (London) **423**, 425 (2003).
[11]K. Takada, H. Sakural, E. Takayama-Muromachi, F. Izumi, R. A. Dilanian, and T. Sasaki, Nature (London) **422**, 53 (2003).
[12]R. E. Schaak, T. Klimczuk, M. L. Foo, and R. J. Cava, Nature (London) **424**, 527 (2003).
[13]M. L. Foo, Y. Wang, S. Watauchi, H. W. Zandbergen, T. He, R. J. Cava, and N. P. Ong, Phys. Rev. Lett. **92**, 247001 (2004).
[14]A. Olariu, P. Mendels, F. Bert, B. G. Ueland, P. Schiffer, R. F. Berger, and R. J. Cava, Phys. Rev. Lett. **97**, 167203 (2006).
[15]M. Hemmida, H. A. Krug von Nidda, N. Büttgen, A. Loidl, L. K. Alexander, R. Nath, A. V. Mahajan, R. F. Berger, R. J. Cava, Y. Singh, and D. C. Johnston, Phys. Rev. B **80**, 054406 (2009).
[16]M. Onoda, J. Phys. Condens. Matter **20**, 145205 (2008).
[17]Y. Tokura and N. Nagaosa, Science **288**, 462 (2000).
[18]H. F. Pen, J. van den Brink, D. I. Khomskii, and G. A. Sawatzky, Phys. Rev. Lett. **78**, 1323 (1997).
[19]M. Giot, L. C. Chapon, J. Androulakis, M. A. Green, P. G. Radaelli, and A. Lappas, Phys. Rev. Lett. **99**, 247211 (2007).
[20]C. Stock, L. C. Chapon, O. Adamopoulos, A. Lappas, M. Giot, J. W. Taylor, M. A. Green, C. M. Brown, and P. G. Radaelli, Phys. Rev. Lett. **103**, 077202 (2009).
[21]T. M. McQueen, P. W. Stephens, Q. Huang, T. Klimczuk, F. Ronning, and R. J. Cava, Phys. Rev. Lett. **101**, 166402 (2008).
[22]J. P. Parant, R. Olazcuaga, M. Devalette, C. Fouassier, and P. Hagenmuller, J. Solid State Chem. **3**, 1 (1971).
[23]R. Hoppe, G. Brachtel, and M. Jansen, Z. Anorg. Allg. Chem. **417**, 1 (1975).
[24]A. Zorko, S. El Shawish, D. Arcon, Z. Jaglicic, A. Lappas, H. van Tol, and L. C. Brunel, Phys. Rev. B **77**, 024412 (2008).
[25]G. R. Zhang, L. J. Zou, Z. Zeng, and H. Q. Lin, J. Appl. Phys. **105**, 07E512 (2009).
[26]Z. W. Ouyang and B. Wang, Phys. Rev. B **82**, 064405 (2010).
[27]W. Tian, M. F. Chisholm, P. G. Khalifah, R. Jin, B. C. Sales, S. E. Nagler, and D. Mandrus, Mater. Res. Bull. **39**, 1319 (2004).
[28]S. J. Clarke, A. J. Fowkes, A. Harrison, R. M. Ibberson, and M. J. Rosseinsky, Chem. Mater. **10**, 372 (1998).
[29]T. Jia, G. Zhang, Z. Zeng, and H. Q. Lin, Phys. Rev. B **80**, 045103 (2009).
[30]P. Blaha, K. Schwarz, G. Madsen, D. Kvasnicka, and J. Luitz, *WIEN2K* (Technische Universitat Wien, Austria, 2007).
[31]J. P. Perdew, K. Burke, and M. Ernzerhof, Phys. Rev. Lett. **77**, 3865 (1996).
[32]S. Yu. Ezhov, V. I. Anisimov, H. F. Pen, D. I. Khomskii, and G. A. Sawatzky, Europhys. Lett. **44**, 491 (1998).
[33]J. B. Goodenough, *Magnetism and the Chemical Bond* (Interscience, New York, 1963).
[34]J. Kanamori, J. Phys. Chem. Solids **10**, 87 (1959).
[35]A. M. Oleś, P. Horsch, L. F. Feiner, and G. Khaliullin, Phys. Rev. Lett. **96**, 147205 (2006).
[36]G. K. Madsen and P. Novák, Europhys. Lett. **69**, 777 (2005).
[37]S. K. Mishra and G. Ceder, Phys. Rev. B **59**, 6120 (1999).
[38]O. I. Velikokhatnyi, C. C. Chang, and P. N. Kumtaa, J. Electrochem. Soc. **150**, A1262 (2003).